Septate junction in the distal ileac plexus of larval lepidopteran *Trichoplusia ni*: alterations in paracellular permeability during ion transport reversal

Dennis Kolosov[1,*], Sima Jonusaite[2], Andrew Donini[3], Scott P. Kelly[3], Michael J. O'Donnell[1]

[1]- McMaster University, Department of Biology, Hamilton, L8S 4K1, Canada

[2]- University of Utah, Division of Nephrology and Hypertension, Department of Internal Medicine, Molecular Medicine Program, Salt Lake City, 84132, USA

[3]- York University, Department of Biology, M3J 1P3, Canada

* corresponding author email: kolosovd@mcmaster.ca

Keywords: septate junctions, Malpighian tubules, Lepidoptera, ion transport reversal, paracellular permeability

Abstract

The Malpighian tubules (MTs) and hindgut together act as the functional kidney in insects. MTs of caterpillars are notably complex and consist of several regions that display prominent differences in ion transport. The distal ileac plexus (DIP) is a region of Malpighian tubule that is of particular interest because it switches from ion secretion to ion reabsorption in larvae fed on ion-rich diets. The pathways of solute transport in the DIP are not well understood, but one potential route is the paracellular pathway between epithelial cells. This pathway is regulated by the septate junctions (SJs) in invertebrates, and in this study, we found regional and cellular heterogeneity in expression of several integral SJ proteins. DIP of larvae fed ion-rich diets demonstrated a reduction in paracellular permeability, coupled with alterations in both SJ morphology and the abundance of its molecular components. Similarly, treatment *in vitro* with helicokinin (HK), an antidiuretic hormone identified by previous studies, altered mRNA abundance of many SJ proteins and reduced paracellular permeability. HK was also shown to target a secondary cell-specific SJ protein Tsp2A. Taken together, our data suggest that dietary ion loading, known to cause ion transport reversal in the DIP of larval *T. ni*, leads to alterations in the paracellular permeability, SJ morphology and its molecular component abundance. The results suggest that HK is an important endocrine factor that co-regulates ion transport, water transport and paracellular permeability in MTs of larval lepidopterans. We propose that co-regulation of all three components of the MT function in larval lepidopterans allows for safe toggling between ion secretion and reabsorption in the DIP in response to variations in dietary ion availability.

Introduction

Ion-transporting epithelia, in general, function in either ion secretion or ion reabsorption in the way they move ions (Reynolds and Bellward, 1989). In contrast, Malpighian tubules (MTs) of lepidopteran larvae are capable of rapid and reversible changes between ion secretion and reabsorption (Kolosov et al, 2018a; Kolosov et al, 2018b; Kolosov and O'Donnell, 2019). These findings suggest that the MT epithelium of larval lepidopterans is capable of rapid self-regulation. Studies aimed at understanding how this happens mechanistically may lead to novel insights into epithelial function. Lepidopteran larvae are economically important crop and forest pests (Sharma et al, 2017) and understanding how their excretory system works may be of use for designing interference strategies targeting this particular group of insects. Similar studies investigating the renal system of dipteran insects have paved the way for insecticide design (reviewed in Beyenbach et al, 2015).

Excretion in insects is accomplished by the MTs and hindgut which together form the functional kidney (Wigglesworth, 1961). The MTs secrete a primary urine by actively transporting ions (Na^+, K^+, Cl^-) from the hemolymph into the tubule lumen, which in turn generates a transepithelial osmotic gradient that facilitates fluid movement (Bradley, 1985). Larval lepidopterans are distinct in that their MTs are not only segmented and specialised in function, but their distal ends are applied to the outer surface of the rectum and enveloped in a perinephric membrane, thus forming the rectal complex (RC) (Ramsay, 1976). The distal ileac plexus (DIP) emerges from the RC – together these two regions are capable of ion and fluid secretion. In contrast the downstream proximal ileac plexus (PIP), and yellow and white regions (YR and WR, respectively) are largely reabsorptive (see **Fig 1A**). The DIP and PIP lie in close proximity to the ileum, whereas the YR and WR run along the surface of the midgut.

Several recent studies have investigated the mechanisms of ion transport in the DIP of *Trichoplusia ni* MT. The DIP contains two types of cells, the principal cells (PCs) and the secondary cells (SCs) (O'Donnell and Ruiz-Sanchez, 2015; Ruiz-Sanchez et al, 2015; Kolosov et al, 2018a; Kolosov et al, 2018b; Kolosov and O'Donnell, 2018; Kolosov et al, 2019; Kolosov and O'Donnell, 2019). SCs are type II cells in the MTs of insects – their dipteran (e.g., mosquito/fly) counterparts are the stellate cells, aptly named because of their shape (Dow, 2012). SCs are named so because they overall take up less of the MT epithelium compared to the fraction taken up by the large polyploid (Type I) PCs (Dow, 2012).

Recent studies have described that ion transport in the DIP of larval *T. ni* can undergo rapid alterations, aimed presumably at ion recycling and recovery. Firstly, the SCs in this region reabsorb K^+ and Na^+ into the hemolymph, while PCs secrete them (O'Donnell and Ruiz-Sanchez, 2015). This ion transport mechanism is thought to be driven, at least in part, by the gap junction-based coupling between the SCs and PCs (Kolosov et al, 2018a). This arrangement is thought to play an important role in making ionoregulation and acid-base balance more efficient in growing larvae (Kolosov and O'Donnell, 2019). Secondly, the DIP is the only region of the free tubule that secretes ions and fluid (Ruiz-Sanchez et al, 2015). However, this region demonstrates significant phenotypic plasticity as it can switch to ion reabsorption when excess ions are supplied through the diet (Kolosov et al, 2018a; Kolosov et al, 2018b; see **Fig 1B**). Thus, the DIP can play an important role in retaining ions by reabsorbing them into the haemolymph. This paradoxical reabsorption *in situ* is thought to be aimed at haemolymph expansion and extraction of ions from the diet by way of the rectal complex and MTs (Kolosov et al, 2018a; Kolosov et al, 2018b; Kolosov and O'Donnell, 2019). Ion reabsorption by the DIP, however, is reversible; when excised and mounted for a Ramsay assay, an isolated DIP promptly reverts to ion secretion (Kolosov et al, 2018a). This likely takes place because of the removal of the DIP from the influence of endocrine factors circulating in the haemolymph and the innate ability of the DIP to autonomously sense changes in luminal ion supply from the rectal complex (Kolosov et al, 2019).

It is likely that a tubule that switches from ion secretion to ion reabsorption will also restrict water permeability and the permeability of the paracellular pathway. Paracellular permeability provides a beneficial fail-safe for a secreting tubule, allowing elimination of any novel xenobiotic for which there is no specific transport mechanism (Maddrell, 1981). But the paracellular permeability also allows back-flux of secreted organic xenobiotics and metabolites from tubule lumen to haemolymph. Therefore, we hypothesize that the DIP in larvae fed ion-rich diets (which reabsorbs ions *in situ*) will likely restrict the permeability of the paracellular pathway between epithelial cells in order to limit detrimental back-flux from the lumen of MTs.

The permeability of the paracellular pathway in the epithelia of invertebrates is regulated by the septate junctions (SJs), a type of occluding cell-cell junction (Jonusaite et al, 2016). In cross-section electron microscopy, SJs display a characteristic ladder-like structure between adjacent cells with septa spanning a 15–20 nm intercellular space (Green and Berquist, 1982). Several morphological variants of SJs exist across invertebrate phyla based on tangentially cut sections and some animals possess multiple types of SJs that are specific to different epithelia (Jonusaite et al, 2016; Green and Berquist, 1982). Molecular analyses of insect SJs have largely been performed in *Drosophila melanogaster*, where two types of SJs are present: the pleated SJ (pSJ) and the smooth SJ (sSJ), which are found in ectodermally and endodermally derived epithelia, respectively (Izumi and Furuse, 2014). To date, over twenty *D. melanogaster* pSJ-associated proteins and three sSJ-specific proteins have been identified, and these include transmembrane and cytoplasmic proteins (Jonusaite et, 2016; Izumi and Furuse, 2014; Deligiannaki et al, 2015; Yanagihashi et al, 2012; Izumi et al, 2012; Izumi et al, 2016). Loss-of-function mutations in most of these proteins prevent the formation of septa or SJ organization, which in turn disrupts the transepithelial barrier properties of the epithelia where they are expressed (Jonusaite et, 2016; Izumi and Furuse, 2014; Furuse and Izumi, 2017). However, our knowledge on the molecular physiology of SJs in other insect species and in particular, how SJs are regulated in different epithelia and/or in response to changes in environmental conditions is scant.

The functional features of the SJ-mediated paracellular pathway in insect MTs have been examined in only a few studies. MTs of *Rhodnius prolixus* are readily permeable to a variety of paracellular permeability markers, such as inulin (~7000 Da), sucrose (342 Da) and polyethylene glycol (PEG; 4000 Da), suggesting a low resistance pathway for molecular flow through septate junctions (O'Donnell et al, 1984; Skaer and Maddrell, 1987). It has been recently reported that the MTs of freshwater larval mosquito *Aedes aegypti* express sSJ-specific proteins snakeskin (Ssk) and mesh which localize to the junctions between all cells (Jonusaite et al, 2017a). In addition, larval tubules express the transmembrane SJ protein gliotactin (Gli) which was confined to the junctional domains between the stellate and principal cells (Jonusaite et al, 2017b). These studies further demonstrated that elevated external salt content caused an increase in Gli protein and Ssk and mesh transcript abundance in larval MTs, which occurred in conjunction with reduced paracellular permeability to PEG-400 (Jonusaite et al, 2017a; Jonusaite et al, 2017b). In MTs of adult *A. aegypti*, the SJs are permselective to Cl^- (Pannabecker et al, 1993). This junctional Cl^- permeability provides a paracellular pathway for Cl^-, allowing it to serve as a counterion for Na^+ and K^+ that are secreted across the epithelium by energy dependent transcellular pathways (Beyenbach and Piermarini, 2011). Paracellular Cl^- permeability in adult *A. aegypti* tubules increases in the presence of the neuropeptide leucokinin-VIII (LKVIII) which in turn increases the transepithelial Na^+, K^+ and fluid secretion (Pannabecker et al, 1993; Yu and Beyenbach, 2001; Yu and Beyenbach, 2004). Moreover, it has been shown that LKVIII changes the MT of adult *A. aegypti* from a moderately tight epithelium (58 Ω cm^2) to a leaky epithelium (10 Ω cm^2) (Pannabecker et al, 1993) and increases junctional permeability to inulin and sucrose (Wang et al, 1996).

To our knowledge, no studies have examined the molecular physiology of SJs in lepidopteran MTs. Recent RNAseq study launched in our lab detected expression of transcripts encoding several SJ proteins in the DIP of larval *T. ni* (Kolosov et al, 2019). We have also demonstrated that ion transport reversal in the DIP is associated with a decrease in transcript abundance of many transcellular ion transport components (Kolosov et al, 2018a) and might be modulated by a lepidopteran kinin, HK (Kolosov and O'Donnell, 2018). With this in mind, the goal of the current study was to identify the molecular components of the septate junction,

profile their expression and quantify changes in their abundance in the DIP of larvae fed ion-rich diets. Simultaneously, we aimed to investigate whether paracellular permeability of the DIP is reduced in larvae fed ion-rich diets, and whether HK can alter paracellular permeability of the DIP as this hormone has been shown to be involved in the regulation of ion and water transport in the DIP. Examination of the molecular components was aimed at identifying potential molecular targets of HK action in the septate junction of *T. ni*.

Methods

Experimental animals

Trichoplusia ni (Hübner, 1800) eggs were purchased from the Great Lakes Forestry Centre (Sault St. Marie, ON). Strain GLfc:IPQL:TniF04 raised (Roe et al, 2018). Larvae were raised at 23–25°C with 40-50% RH and fed synthetic McMorran diet (McMorran, 1965), containing $[K^+]$=59mM and $[Na^+]$=18mM. Feeding fifth instar larvae were used for all experiments. Larvae were dissected in standard lepidopteran saline (O'Donnell and Ruiz-Sanchez, 2015; Maddrell and Gardiner, 1976) (in mM); 15 NaCl, 30 KCl, 2 $CaCl_2$, 30 $MgCl_2$, 10 $KHCO_3$, 5 $KHPO_4$, 10 glucose, 10 maltose, 5 trisodium citrate, 10 glycine, 10 alanine, 10 proline, 10 glutamine, 10 valine, 5 serine, 5 histidine, pH=7.2.

Ion-rich diets

Diets rich in K^+ (200 mM, 'High-K^+') or Na^+ (60 mM, 'High-Na^+') were prepared by adding KCl or NaCl, respectively, to standard lepidopteran diet (see above) prior to mixing and pouring into diet cups. A survey of crops that *Trichoplusia* feed on confirmed that these ion levels in the diet are physiologically relevant (source: https://ndb.nal.usda.gov/). Diets were thoroughly mixed and set into individual diet cups, allowed to solidify at room temperature, capped with sterilized lids and refrigerated until use. Larvae were fed on these diets as 5th instars for 24h.

RNA extraction, cDNA synthesis and expression profile PCR amplification

RNA extraction, cDNA synthesis and PCR amplification were performed as previously described (Kolosov et al, 2018a; Kolosov et al, 2018b, Kolosov and O'Donnell, 2018). Briefly, larvae were dissected in lepidopteran saline and tissues of interest such as the rectal complex (RC, containing cryptonephridial tubule), the distal ileac plexus (DIP), the proximal ileac plexus (PIP), the yellow region (YR) and the white region (WR) of the Malpighian tubule were separated. Three samples from individual caterpillars were pooled to avoid reporting undetected transcript based on its absence from a single animal. Distinct regions of the free tubule were sampled from all six tubules of every caterpillar. Tissues were homogenized in Trizol® and total RNA was extracted using the manufacturer's protocol.

Following RNA extraction, 2 μg of total RNA were treated with DNAse and used for cDNA synthesis with oligo-dT-aided reverse-transcriptase. cDNA was serially-diluted in RNAse/DNAse-free water and used for PCR. SJ-specific primers were designed based on sequences obtained from *Trichoplusia ni* genomic transcriptome. PCR amplicons were sequenced to confirm identity and submitted to GenBank for annotation (see Table 1 for PCR primer and cycling information).

Whole-mount immunohistochemical detection of TSP2A

Whole-mount immunohistochemistry (IHC) on the DIP of the larval *T. ni* was performed as previously described[6]. Briefly, DIPs from 5th instar larvae were dissected in lepidopteran saline and fixed in 4% paraformaldehyde (PFA) in phosphate-buffered saline (PBS, pH = 7.4) overnight at 4°C. DIPs were then washed in PBS and dehydrated (20%, 40%, 60%, 80% and 100%, v/v) and rehydrated in methanol/PBS series (100% → PBS). DIPs were then permeabilized and blocked in 0.1% Triton X-100 PBS solution (PBT), containing 2% bovine serum albumin w/v (BSA) at room temperature for 2 hours. Primary antibody incubation was performed overnight at 4°C at 1:100 dilution in PBT/1%-BSA. Tsp2A was localized using a custom-synthesized polyclonal antibody raised against *Drosophila* Tsp2A in rabbit and generously donated by Dr. Mikio Furuse (National Institute for Physiological Sciences, Japan). The peptide corresponds to amino acid residues of the cytosolic C-terminal domain of *Drosophila* Tsp2A NH_2-CAVKKEEEQASNYRR-COOH[16]. Comparison of epitope sequence to Tsp2A found in *Trichoplusia* demonstrated 86% sequence

identity. An additional preparation was included with each IHC analysis, where primary antibody was omitted to act as negative control. Tissues were washed after 16–18h in PBT/1%-BSA supplemented with normal goat serum 3 times for 15min each with constant agitation to remove unbound primary antibody. Following washes, tissues were incubated with 1:1000 of secondary goat anti-rabbit TRITC-conjugated secondary antibody (Cedarlane, Burlington, ON, Canada) in the dark at room temperature for 2h. Following incubation with secondary antibody, tissues were washed 3 times in PBT/1%-BSA for 15min each time. Tubules were then mounted on slides using a transfer pipet. Slides were then blotted dry using KimWipes and preparations were mounted using ProLong Antifade® reagent (ThermoFisher Scientific) containing DAPI as a nuclear stain under coverslips and left to cure in the dark. Images were obtained using a laser-scanning confocal image acquisition system CTR-6500 coupled to a Leica DM6000CS microscope at McMaster University imaging facilities.

In vitro exposure to helicokinin

Synthetic helicokinin (HK; $YFSPWG_{amide}$) used in this study was purchased from GenScript (Piscataway, NJ, USA) and paired experiments were conducted on the DIP isolated from larvae fed control diet and pre-treated with 10^{-8} M HK, as described previously (Kolosov and O'Donnell, 2018). Briefly, two DIPs were dissected out from the same larva. One was placed in a Petri dish with saline, while the other was placed in another Petri dish containing 10^{-8} M HK in the same batch of saline. The sham control was treated with an equal amount of saline used to deliver HK to the experimental group. Tubules were treated with HK or saline at room temperature for 4 h. After the incubation period paired samples were randomly assigned for qPCR analysis or paracellular permeability assays.

Paracellular permeability assay

Excised DIPs were mounted for a typical Ramsay assay (see **Fig 3A**) in a saline droplet. After secreting for 15 min, a droplet was collected and used as an initial sample to account for background fluorescence in the secreted fluid. Following this, 4 kDa FITC-dextran dissolved in saline, was added to the droplet for a final concentration of 3 mg/ml. This protocol ensured that: (i) the tubule was intact and secreting at a constant rate, and (ii) the end of the tubule,

where secreted fluid would be collected from, was not immersed in FITC-dextran during mounting. Dextran concentration was measured as follows: droplets of secreted fluid were collected and sized using an ocular micrometer. Droplets were then added to 50-µl of lepidopteran saline. Samples were loaded into dark plates and FITC-dextran concentration was measured in every sample using a Synergy 2 BioTek microplate reader (Winooski, VT), along with a standard curve. The concentration of FITC-dextran in the original secreted droplet was then calculated by accounting for the dilution factor (original droplet volume + 50 µl)/original droplet volume.

Transcript abundance measurements using qPCR

SJ protein transcript abundance in larval *T. ni* tissues was examined using quantitative real-time PCR (qPCR). qPCR analysis was carried out using EvaGreen 5x qPCR Mastermix (DiaMed Lab Supplies Inc, Mississauga, ON, Canada) in a BioRad CFX Connect qPCR machine (San Diego, California, USA). Primer sets used for PCR detection were used for qPCR quantification. The following reaction conditions were used: 1 cycle for denaturation (95 °C, 4 min), then 40 cycles of: denaturation (95 °C, 30 s), annealing (see Table 1, 30 s) and extension (72 °C, 30 s), with a final extension step (72 °C, 10 min). To ensure that a single PCR product was synthesized during reactions, a melting curve analysis was carried out after each qPCR run. Transcript abundance was normalized to that of *Trichoplusia* tubulin (*tub*). The use of *tub* for gene of interest normalization in dietary ion loading studies was validated by statistically comparing *tub* threshold cycle values between tissues originating from animals raised on different diets to confirm that no statistically significant changes occurred in different groups as a result of dietary treatment ($P = 0.840$, One-way ANOVA). Similar analysis was performed for the HK-treated tissues ($P=0.502$, Student's t-test).

Transmission electron microscopy and septate junction morphology

Samples of DIP from larvae fed control, high-K^+ and high-Na^+ diets were dissected out and fixed in 2% glutaraldehyde and 4% paraformaldehyde in lepidopteran saline. The samples were then rinsed in saline, post-fixed in 1% osmium tetroxide and dehydrated in a graded ethanol series followed by propylene oxide. The tissues were embedded in Quetol-Spurr resin. Sections of 90 nm thickness were cut on a Leica Ultracut ultramicrotome, stained with uranyl acetate and lead citrate and viewed using a Tecnai 20 TEM (FEI, Hillsboro, OR, USA) at NanoScale Biomedical Imaging Facility (The Hospital for Sick Children Research Institute, Toronto, Canada). Septate junction morphology was described using apparent length and convolutedness as morphology criteria. Small sample size and lack of access to a local TEM precluded statistical analysis of significant differences.

Statistical analysis

Significant differences due to experimental treatment were determined using a Student's t-test or a one-way ANOVA, followed by a Holm-Sidak post-hoc test as indicated in figure captions. All the statistical tests were performed in SigmaPlot (version 11) statistical software, which runs t-test and ANOVA alongside normality and equal variance tests. Significance was based on the observation of a $p<0.05$.

Data availability

All data and images described in the manuscript will be uploaded to FigShare upon acceptance of the manuscript and are available from the corresponding author on reasonable request.

Results

SJ protein genes demonstrate heterogeneous expression in the regions and cell types of the MT of larval *T. ni*

Transcripts encoding for the SJ genes *kune*, *mega* and *tsp2A* were detected in all regions of the MT examined in this study which included the rectal complex (RC, containing cryptonephric tubule and rectal epithelium), distal ileac plexus (DIP), proximal ileac plexus (PIP), and the yellow and white regions (YR and WR) of the MT in larval *T. ni* (**Fig 1 C-E**). However, mRNA expression of SJ genes encoding for *nrxIV*, *sinu* and *mesh* was restricted to the RC, DIP and PIP regions (**Fig 1 F-H**). This observation highlights heterogeneous expression of SJ transcripts along the length of the MT. Additionally, immunohistochemical analysis of Tsp2A in the DIP of *T. ni* larvae revealed that Tsp2A immunolocalization was confined to the cell-cell contact regions between the secondary and principal cells (**Fig 2A-B**). This confined localization was confirmed in another preparation, which although redundant was included in the figure to highlight experimental repeatability (**Fig 2C-D**). In contrast, no Tsp2A immunoreactivity was observed in the cell-cell contact region between two adjacent principal cells (**Fig 2A-D**). No Tsp2A immunoreactivity was observed in control whole mounts that had been probed with secondary antibody only (**Fig 2E-F**). Both observations demonstrate that SJ transcript and protein expression exhibits regional and cellular heterogeneity in expression in the MT of larval lepidopterans.

Effects of ion-rich diet on SJ gene transcript abundance in the DIP

Previous studies have reported that DIP of *T. ni* larvae fed ion-rich diets reabsorbs K^+ instead of secreting it. In order to investigate whether the paracellular permeability and its molecular components are also affected by ion-rich diets, we measured SJ mRNA abundance and paracellular permeability. The DIP showed a significant decrease in transcript abundance of all SJ genes examined, i.e. *kune*, *mega*, *mesh*, *nrxIV*, *sinu* and *tsp2A* (**Fig 3A-F**, High-K^+). Similarly, transcript abundance of *mega*, *mesh*, *sinu* and *tsp2A* also decreased in the DIPs from larvae fed high-Na^+ diet compared to control group (**Fig 3A-F**, High-Na^+). Feeding *T. ni* larvae ion-rich diets was also accompanied by reduced paracellular permeability to 4 kDa FITC-dextran in the DIP

(**Fig 4B**, 0.036 ± 0.007 mg/ml for high-K^+ and 0.035 ± 0.006 mg/ml for high-Na^+ compared to the value for the DIP of control-fed larvae, 0.154 ± 0.021 mg/ml).

Effects of 10^{-8} M helicokinin (HK) on the paracellular permeability and SJ mRNA abundance in the DIP

Previous studies in larval lepidopterans and other insects have implicated kinins in the regulation of paracellular permeability of the MTs. In addition, HK was specifically implicated in the reduction of water permeability, K^+ secretion, and mRNA abundance of secretory ion transporters in the DIP of the larval *T. ni* (Kolosov and O'Donnell, 2019) In order to investigate whether HK also affects paracellular permeability and mRNA abundance of SJ proteins, we incubated isolated DIP of control-fed larvae with 10^{-8} M HK. Upon this exposure, the DIP showed a significant reduction in paracellular permeability to FITC-dextran (0.094 ± 0.010 mg/ml compared to sham-incubated control-fed larvae 0.154 ± 0.021 mg/ml) (**Fig 4B**). Treatment of DIPs isolated from larvae fed control diet with 10^{-8} M helicokinin resulted in elevated mRNA abundance of *mega*, *mesh*, *nrxIV* and *tsp2A*, while transcript abundance of *sinu* decreased (**Fig 5**).

Effects of ion rich diet on SJ ultrastructure in the DIP epithelium

In order to investigate whether the reduction in paracellular permeability and SJ mRNA abundance in the DIP of larvae fed ion-rich diet were accompanied by alterations in SJ morphology, ultrathin sections were analysed by electron microscopy. This revealed smooth SJs in the regions of cell-cell contact between principal cells (PCs) as well as PCs and secondary cells (SCs) (**Fig 6**). Feeding *T. ni* larvae ion-rich diets resulted in the alteration of SJ morphology between the PCs of DIP epithelium (**Fig 6**). In high-magnification images, SJs between two PCs in the DIP of larvae fed high-K^+ and high-Na^+ diets appeared longer and more convoluted than SJs in the DIP of control-fed larvae (**Fig 6**). Similarly, the SJs between the PC and SC revealed SJ that appeared longer (**Fig 7**).

Discussion

Overview and significance

In general, MTs of insects can generate extreme solute concentration gradients (up to 3000:1 between lumen and haemolymph) and may maintain transepithelial potential exceeding 100 mV (Skaer and Maddrell, 1987). These features require a paracellular pathway sufficiently tight to minimize diffusive back-flux of secreted solutes. The main goal of this study was to investigate whether the region of MTs in larval lepidopterans that switches from ion secretion to ion reabsorption simultaneously restricts the paracellular permeability. We hypothesized that this would be beneficial in minimizing the harmful back-flux of secreted organics that would occur in the segment of the tubule that is now reabsorptive. In addition, we hypothesized that the neuropeptide helicokinin (HK) may be involved in the regulation of paracellular permeability of lepidopteran MTs as insect kinins have been demonstrated to alter paracellular permeability of MTs by previous studies. Our results demonstrate that (i) paracellular permeability, (ii) SJ morphology and (iii) transcript abundance of several integral SJ proteins were altered in the DIP of *T. ni* larvae fed ion-rich diet. Neuropeptide HK is likely involved in this process, as treatment with 10^{-8} M HK induces a reduction in paracellular permeability and alterations in SJ transcript abundance in the DIP of control-fed larvae. We have previously shown that HK regulates active ion transport and water permeability in the MTs of lepidopteran larvae. Therefore, results presented in the current study identified HK as a common endocrine link in the regulation of paracellular permeability and transcellular ion transport in the DIP of lepidopteran larvae. Additionally, the current study is the first to report on the molecular components of SJs in the MTs of lepidopteran larvae.

Expression of SJ mRNA and transcript demonstrate regional and cellular heterogeneity in the architecturally complex MT of larval lepidopterans

MTs of larval lepidopterans exhibit regional heterogeneity in ion transport, water permeability and luminal ion content (Moffett, 1994; O'Donnell and Ruiz-Sanchez, 2015; Ruiz-Sanchez et al, 2015). In isolated preparations of the free *T. ni* MTs, the DIP is the main fluid secretory segment, while the downstream regions of the tubule (PIP, YR and WR) do not contribute to fluid secretion (Ruiz-Sanchez et al, 2015). The current study revealed that expression of SJ transcripts and protein is similarly heterogeneous in a region- and cell type-specific manner in two of the following ways.

Firstly, regional heterogeneity in SJ expression may indicate that a similar heterogeneity in paracellular permeability exists in different regions of the MTs. In the current study, many SJ transcripts were absent from YR and WR, the two regions that are notably missing many secretory ion pumps and transporters (Kolosov et al, 2018b). YR and WR are also known to have lower luminal pH used to drive precipitation of ammonium urate and potassium urate crystals in the lumen. This is likely achieved via base reabsorption into the haemolymph and/or the adjacent midgut (Onken and Moffett, 2017). How this happens mechanistically is largely unknown. However, in the YR and WR, which do not seem to contribute to ion and fluid secretion (Ruiz-Sanchez et al, 2015; Kolosov et al, 2018b), an epithelium with leaky SJs would be disadvantageous. Therefore, the absence of *mesh, nrxIV* and *sinu* gene transcripts in the YR and WR of larval *T. ni*, as shown in this study, may be indicative of a tight epithelium in these regions. Tissue-specific expression and changes in SJ mRNA transcript abundance have been correlated with alterations in paracellular permeability of insect epithelia (Jonusaite et al, 2016; Jonusaite et al, 2017a). However, further studies will be required to substantiate this claim as we cannot rule out the possibility of the presence of other yet unidentified SJ components in the YR and WR of *T. ni* larva.

Secondly, the presence of Tsp2A exclusively at the PC-SC contact in the DIP may indicate an enhanced paracellular barrier around the SCs (**Fig 2A-D**). It is worth noting that SCs of *T. ni* have been shown to express multidrug resistance proteins (MRPs) and were suggested to be a hotspot for excretion of xenobiotics and plant-based diet-derived toxins (Labbe et al, 2011).

MRPs are ATPases that actively drive excretion of xenobiotics and can establish a significant concentration gradient across the region of the tubule where these proteins are expressed (Dow and Davies, 2006). Thus, the association of Tsp2A with SCs of the DIP of larval *T*. *ni* may provide a functional link between xenobiotic excretion by this region of the MT and its paracellular barrier function in this insect. In *D*. *melanogaster*, Tsp2A is required for the paracellular barrier function in the midgut (Izumi et al, 2016). Similarly, multiple reports of SC-specific protein expression exist in dipteran MTs (reviewed in Dow, 2012).

Observations that, (i) YR and WR, which do not contribute to ion and fluid secretion, express fewer SJ transcripts, and (ii) Tsp2A localization surrounding SCs, which are thought to actively transport xenobiotics, suggest that actively transporting regions of the tubule may differ in paracellular permeability from adjacent regions that do not exhibit active ion transport.

A less leaky epithelium minimizes the detrimental back-flux of organics from the lumen into the haemolymph in larvae fed ion-rich diets

It has been suggested that even though the SJ can be leaky, if the rate of active ion transport in the secretory segment of insect tubule sufficiently exceeds the paracellular backflux, the epithelium will, overall, show a 'tight' phenotype (O'Donnell and Maddrell, 1984; Skaer and Maddrell, 1987). Previous work has demonstrated that the DIP is the only region that contributes to ion and fluid secretion in isolated MTs of the larval *T. ni* (O'Donnell and Ruiz-Sanchez, 2015; Ruiz-Sanchez et al, 2015). Importantly, the DIP was shown to express an abundance of xenobiotic transporters (Labbé et al, 2011; Kolosov et al, 2019). Higher paracellular permeability in a secreting tubule has been suggested to provide a fail-safe for excretion of novel xenobiotics and toxins (Maddrell, 1981). Higher passive permeability of a secreting tubule allows the insect to flush xenobiotics and toxins from the haemolymph by increasing the fluid secretion rate. This is applicable if the xenobiotic/toxin in question is (i) novel and the tubules don't yet have a well-developed and dedicated active transporter system for it and/or (ii) the toxin is present at concentrations in the haemolymph that are too high to be eliminated by employing active transporter systems. However, DIP of *T*. *ni* larvae fed ion-rich diets reduces the rate of K^+ secretion, or switches to K^+ reabsorption (Kolosov et al, 2018a;

Kolosov et al, 2018b). Therefore, a reduction in paracellular permeability may minimize the diffusive back-flux of inorganic ions and secreted toxins back into the haemolymph in the DIP, which now reabsorbs ions (and presumably fluid).

In this study we demonstrated that in the DIP of larvae fed high-Na^+ or high-K^+ diet: (i) paracellular permeability was reduced, coinciding with (ii) the appearance of longer and more convoluted SJs between the epithelial cells of the DIP, as well as (iii) decreased mRNA abundance of most SJ proteins examined. Similar appearances of convoluted SJs are associated with a decrease in paracellular permeability in the midgut of *Drosophila* (MacMillan et al, 2017) and crab gill epithelium (Luquet et al, 1997; Luquet et al, 2002). Loss-of-function mutations in *kune*, *mega*, *mesh*, *nrxIV*, *sinu,* and *tsp2A* are associated with the functional disruption of the paracellular barrier and SJ integrity in *Drosophila* epithelia (Jonusaite et al, 2016), indicating the importance of these proteins in insect SJs. However, the roles of individual SJ proteins in the regulation of paracellular permeability remain largely unknown. For instance, increase in *mesh* mRNA transcript abundance coinciding with increased paracellular permeability of the midgut in response to elevated salinity has been reported for larval *A*. *aegypti* (Jonusaite et al, 2017a; Jonusaite et al, 2016). In contrast, rearing *A*. *aegypti* larvae in brackish water increased *mesh* transcript abundance in the MTs, coinciding with decreased paracellular permeability of the epithelium (Jonusaite et al, 2017a).

Taken together, our observations of changes in mRNA transcript abundance of SJ genes, reduced paracellular permeability, and altered SJ morphology in the DIP of larvae fed ion-rich diets, suggests that restructuring of the SJ is an important part of the switchover from ion secretion to ion reabsorption.

Helicokinin reduces paracellular permeability in MTs of larval Lepidoptera

In the MTs of adult dipterans (mosquitoes and flies), treatment with kinin increases permeability to Cl^- and reduces transepithelial potential (Beyenbach and Piermarini, 2011; Yu and Beyenbach, 2001; Beyenbach, 2003; O'Donnell et al, 1996; Cabrero et al, 2014). In *A. aegypti* MTs, kinin stimulated Cl^- transport has been proposed to occur through a paracellular shunt provided by the SJs between the PCs and SCs (Beyenbach and Piermarini, 2011). In the

current study we demonstrated that HK reduced paracellular permeability of the DIP of larval *T. ni* (**Fig 4B**) and increased transcript abundance of *mega*, *mesh*, *nrxIV* and *tsp2A*, while reducing mRNA abundance of *sinu* (**Fig 5**). It is important to point out that mRNA abundance of Tsp2A, which localizes to the SJs between the PC and SC (**Fig 2**), increased in HK-treated DIPs. This suggests HK-mediated regulation of SJ function in lepidopteran MTs. As mentioned earlier, in MTs of adult *A. aegypti*, leucokinin (LK) opens up a paracellular shunt pathway for the secretion of Cl^- and also increases junctional permeability to inulin and sucrose (Beyenbach and Piermarini, 2011; Wang et al, 1996). In contrast, in MTs of *Drosophila*, drosokinin acts on the transcellular pathway by opening up chloride channels in SCs (O'Donnell et al, 1996; Cabrero et al, 2014). HK, which in the current study reduced paracellular permeability of the lepidopteran DIP, provides yet another example of kinin action on lepidopteran MTs that differs greatly from its effect on the dipteran MTs. Previous studies have described HK as an antidiuretic capable of changing $[Na^+]/[K^+]$ ratio of the secreted fluid and reducing *aqp-1* abundance in the DIP of the larval *T. ni* (Kolosov and O'Donnell, 2018; Kolosov and O'Donnell, 2019). Therefore, it appears that despite the previously reported differences in the action of HK and LK on ion and water transport by MTs of lepidopterans and dipterans, respectively (Kolosov and O'Donnell, 2018; Yu and Beyenbach 2001; Cabrero et al, 2014), SC-based SJs may be a conserved target of kinins in both insect orders. It is also worth pointing out that the effects of HK on the paracellular permeability of the DIP cannot be explained by the observed changes in transcript abundance of SJ proteins alone. This is likely the case because because the effects of HK on the transcript abundance of SJ protein mRNA are in many cases different from those of ion-rich diets. In fact, the observed changes are likely to be a part of a long-term response - a molecular restructuring of the SJ - in response to HK.

Conclusions and implications

SJs define the properties of the paracellular pathway in insect MTs, but our understanding of the contribution of this pathway to internal homeostasis as well as its regulation and the mechanism of action of hormonal factors remains elusive. This study provides insight into the molecular SJ architecture of MTs of larval Lepidoptera. These MTs are noteworthy because they

can change the direction of ion transport rapidly and reversibly (Kolosov et al, 2018a; Kolosov et al, 2018b; Kolosov and O'Donnell, 2019). These changes would require alterations in water permeability and paracellular junction permeability aimed at preventing passive diffusive back-flux of water and organics/xenobiotics out of the tubule once it stops secreting. In previous studies we have demonstrated that neuropeptide HK mediates the reduction in active ion transport and water permeability in the DIP of larvae fed ion-rich diets (Kolosov and O'Donnell, 2018; Kolosov and O'Donnell, 2019). In the current study, we provide direct evidence that alterations in dietary ion content also have profound effects on paracellular permeability of the MTs. Importantly, we have demonstrated that HK reduces paracellular permeability of MTs in larval lepidopterans. Further electrophysiological studies as well as investigations of the functions of SJ proteins are needed to reveal the functional characteristics of the SJ complex and mechanisms that couple kinin to the modulation of junctional permeability of larval lepidopteran DIP during ion transport reversal.

Acknowledgements and Funding

The authors thank Doug Holmyard (Advanced Bioimaging Centre, Sick Kids Hospital Research Institute, Toronto, ON, Canada) for assistance with the electron microscopy. This work was supported by Natural Sciences and Engineering Research Council of Canada (NSERC) Discovery grants to MJO, AD and SPK, an NSERC Postdoctoral Fellowship to DK.

Author contributions statement

D.K., S.J. and M.J.O. conceived the study. D.K. and S.P.K. collected the data. D.K. analyzed the data. D.K. drafted the manuscript, all authors edited the manuscript.

Competing interests

The authors declare no competing interests.

References

Beyenbach, K. W. (2003). Transport mechanisms of diuresis in Malpighian tubules of insects. *J. Exp. Biol.* **206**, 3845–3856.

Beyenbach, K. W., & Piermarini, P. M. (2011). Transcellular and paracellular pathways of transepithelial fluid secretion in Malpighian (renal) tubules of the yellow fever mosquito *Aedes aegypti*. *Acta Physiologica*, **202**, 387–407.

Beyenbach, K. W., Yu, Y., Piermarini, P. M., & Denton, J. (2015). Targeting renal epithelial channels for the control of insect vectors. *Tissue Barriers*, *3*(4), e1081861.

Bradley, T.J. (1985). Comprehensive Insect Physiology: Biochemistry and Pharmacology (ed. Kerkut, G. A. and Gilbert) pp. 421–465 (Pergamon Press).

Cabrero, P., Terhzaz, S., Romero, M. F., Davies, S. A., Blumenthal, E. M., Dow, J. A. (2014). Chloride channels in stellate cells are essential for uniquely high secretion rates in neuropeptide stimulated Drosophila diuresis. Proc. Nat. Acad. Sci. USA **111**, 14301-14306.

Deligiannaki, M., Casper, A. L., Jung, C. & Gaul, U. (2015). Pasiflora proteins are novel core components of the septate junction. Dev. **142** (17), 3046–3057.

Dow, J. A. T., & Davies, S. A. (2006). The Malpighian tubule: Rapid insights from post-genomic biology. *J. Insect Physiol.* **52**, 365–378.

Dow, J. A. T. (2012). The versatile stellate cell - more than just a space-filler. *Journal of Insect Physiology*, *58*(4), 467–472.

Furuse, M. & Izumi, Y. (2017). Molecular dissection of smooth septate junctions: understanding their roles in arthropod physiology. *Ann. NY Acad. Sci.* **1397**, 17-24.

Green, C. R. & Bergquist, P. R. (1982). Phylogenetic relationships within the invertebrates in relation to the structure of septate junctions and the development of 'occluding' junctional types. *J. Cell Sci.* **53**, 279–305.

Izumi, Y., Yanagihashi, Y., Furuse, M. (2012). A novel protein complex, Mesh-Ssk, is required for septate junction formation in the *Drosophila* midgut. *J. Cell Sci.* **125** 4923–4933.

Izumi, Y. & Furuse, M. (2014). Molecular organization and function of invertebrate occluding junctions. *Semin. Cell Dev. Biol* **36**, 186-193.

Izumi, Y., Motoishi, M., Furuse, K., & Furuse, M. (2016). A tetraspanin regulates septate junction formation in Drosophila midgut. *J. Cell Sci*. **129**, 1155–1164.

Jonusaite, S., Donini, A., & Kelly, S. P. (2016). Occluding junctions of invertebrate epithelia. *J. Comp. Physiol. B* **186**, 17–43.

Jonusaite, S., Kelly, S. P., & Donini, A. (2016). The response of claudin-like transmembrane septate junction proteins to altered environmental ion levels in the larval mosquito *Aedes aegypti*. *J. Comp. Physiol. B* **186**, 589–602.

Jonusaite, S., Donini, A., & Kelly, S. P. (2017a). Salinity alters snakeskin and mesh transcript abundance and permeability in midgut and Malpighian tubules of larval mosquito, *Aedes aegypti*. *Comp. Biochem. Physiol. A* **205**, 58–67.

Jonusaite, S., Kelly, S. P., & Donini, A. (2017b). Identification of the septate junction protein gliotactin in the mosquito *Aedes aegypti*: evidence for a role in increased paracellular permeability in larvae. *J. Exp. Biol.* **220**, 2354–2363.

Kolosov, D., Piermarini, P. M., & O'Donnell, M. J. (2018a). Malpighian tubules of *Trichoplusia ni*: recycling ions via gap junctions and switching between secretion and reabsorption of Na^+ and K^+ in the distal ileac plexus. *J. Exp. Biol*. **221**, jeb172296 10.1242/jeb.172296.

Kolosov, D., Tauqir, M., Rajaruban, S., Piermarini, P. M., Donini, A., & O'Donnell, M. J. (2018b). Molecular mechanisms of bi-directional ion transport in the Malpighian tubules of a lepidopteran crop pest, *Trichoplusia ni*. *J. Insect Physiol.* **109**, 55–68.

Kolosov, D., & O'Donnell, M. J. (2018). Helicokinin alters ion transport in the secondary cell-containing region of the Malpighian tubule of the larval cabbage looper Trichoplusia ni. *Gen. Comp. Endocr.* 10.1016/j.ygcen.2018.07.005.

Kolosov, D., Donly, C., MacMillan H. A., O'Donnell M.J. (2019). Transcriptomic analysis of the Malpighian tubule of *Trichoplusia ni*: clues to mechanisms for switching from ion secretion to ion reabsorption in the distal ileac plexus. *J. Insect Physiol.* **112**, 73-89.

Kolosov, D., O'Donnell M.J. (2019). The Malpighian tubules and cryptonephric complex in lepidopteran larvae. *Adv. Insect Physiol.* In press, https://doi.org/10.1016/bs.aiip.2019.01.006

Labbe, R., Caveney, S., & Donly, C. (2011). Expression of multidrug resistance proteins is localized principally to the Malpighian tubules in larvae of the cabbage looper moth, *Trichoplusia ni*. *J. Exp Biol.* **214**, 937–944.

Luquet, C., Pellerano, G., & Rosa, G. (1997). Salinity-induced changes in the fine structure of the gills of the semiterrestrial estuarian crab, *Uca uruguayensis* (Nobili, 1901) (Decapoda, Ocypodidae). *Tissue Cell* **29**, 495–501.

Luquet, C., Genovese, G., Rosa, G., & Pellerano, G. (2002). Ultrastructural changes in the gill epithelium of the crab *Chasmagnathus granulatus* (Decapoda: Grapsidae) in diluted and concentrated seawater. *Mar. Biol.* **141**, 753–760.

MacMillan, H. A., Yerushalmi, G. Y., Jonusaite, S., Kelly, S. P., & Donini, A. (2017). Thermal acclimation mitigates cold-induced paracellular leak from the Drosophila gut. *Nature Publishing Group*, **7**, 8807 10.1038/s41598-017-08926-7.

Maddrell, S.H. & Gardiner, B.O. (1976). Excretion of alkaloids by malpighian tubules of insects. *J. Exp. Biol*. **64**, 267–281.

Maddrell, S.H. (1981). The Functional Design of the Insect Excretory System. *J. Exp. Biol.*, **90,** 1-15.

McMorran, A. (1965). A synthetic diet for the spruce budworm, *Choristoneura fumiferana* (Clem.) (Lepidoptera: Tortricidae). *Can. Entomol*. **97**, 58–62.

Moffett, D. F. (1994). Recycling of K^+, Acid-Base Equivalents, and Fluid between Gut and Hemolymph in Lepidopteran Larvae. *Physiol. Zool.* **67**, 68–81.

O'Donnell, M. J., Maddrell, S. H., & Gardiner, B. O. (1984). Passage of solutes through walls of Malpighian tubules of *Rhodnius* by paracellular and transcellular routes. *Am. J. Physiol*. **246**, R759–69.

O'Donnell, M. J., Dow, J. A., Huesmann, G. R., Tublitz, N. J., & Maddrell, S. H. (1996). Separate control of anion and cation transport in malpighian tubules of *Drosophila melanogaster*. *J. Exp. Biol.* **199**, 1163–1175.

O'Donnell, M. J., & Ruiz-Sanchez, E. (2015). The rectal complex and Malpighian tubules of the cabbage looper (*Trichoplusia ni*): regional variations in Na^+ and K^+ transport and cation reabsorption by secondary cells. *J. Exp. Biol.* **218**, 3206–3214.

Onken, H. and Moffett, D. F. (2017). Acid-Base Loops in Insect Larvae with Extremely Alkaline Midgut Regions in *Acid-Base Balance and Nitrogen Excretion in Invertebrates* (ed. Weihrauch, D. & O'Donnell, M. J.) pp. 239–260 (Springer).

Pannabecker, T. L., Hayes, T. K., & Beyenbach, K. W. (1993). Regulation of Epithelial Shunt Conductance by the Peptide Leucokinin. *J. Membr. Biol*. **132**, 63–76.

Ramsay, J.A. (1976). The rectal complex in the larvae of lepidoptera. *Philos. Trans. R. Soc. Lond. B Biol. Sci.* **274**, 203–226.

Reynolds, S.E., & Bellward, K. (1989). Water-Balance in Manduca-Sexta Caterpillars - Water Recycling From the Rectum. *J. Exp. Biol.* **141**, 33–45.

Roe, A. D., Demidovich, M., & Dedes, J. (2018). Origins and History of Laboratory Insect Stocks in a Multispecies Insect Production Facility, With the Proposal of Standardized Nomenclature and Designation of Formal Standard Names. *J. Insect Sci.* **18**, 474–9.

Ruiz-Sanchez, E., O'Donnell, M. J., & Donini, A. (2015). Secretion of Na(+), K(+) and fluid by the Malpighian (renal) tubule of the larval cabbage looper *Trichoplusia ni* (Lepidoptera: Noctuidae). *J. Insect Physiol.* **82**, 92–98.

Sharma, S., Kooner, R., & Arora, R. (2017). Insect Pests and Crop Losses. In *Breeding Insect Resistant Crops for Sustainable Agriculture* (pp. 45-66). Springer, Singapore.

Skaer, H. L. & Maddrell, S. (1987). How Are Invertebrate Epithelia Made Tight. *J. Cell Sci.* **88**, 139–141.

Yanagihashi, Y., Usui, T., Izumi, Y., Yonemura, S., Sumida, M., Tsukita, S., Uemura, T., Furuse, M. (2012). Snakeskin, a membrane protein associated with smooth septate junctions, is required for intestinal barrier function in Drosophila. *J. Cell Sci.* **125**, 1980–1990.

Yu, M. J. & Beyenbach, K. W. (2001). Leucokinin and the modulation of the shunt pathway in Malpighian tubules. *J. Insect Physiol.* **47**, 263–276.

Yu, M. J. & Beyenbach, K. W. (2004). Effects of leucokinin-VIII on *Aedes* Malpighian tubule segments lacking stellate cells. *J. Exp. Biol.* **207**, 519-526.

Wang, S., Rubenfeld, A. B., Hayes, T. K. & Beyenbach, K. W. (1996). Leucokinin increases paracellular permeability in insect Malpighian tubules. *J. Exp. Biol.* **199**, 2537-2542.

Wigglesworth, V.B. (1961). The principles of insect physiology (5th Ed), 279, pp. 367-373. (Methuen & Co).

Figures

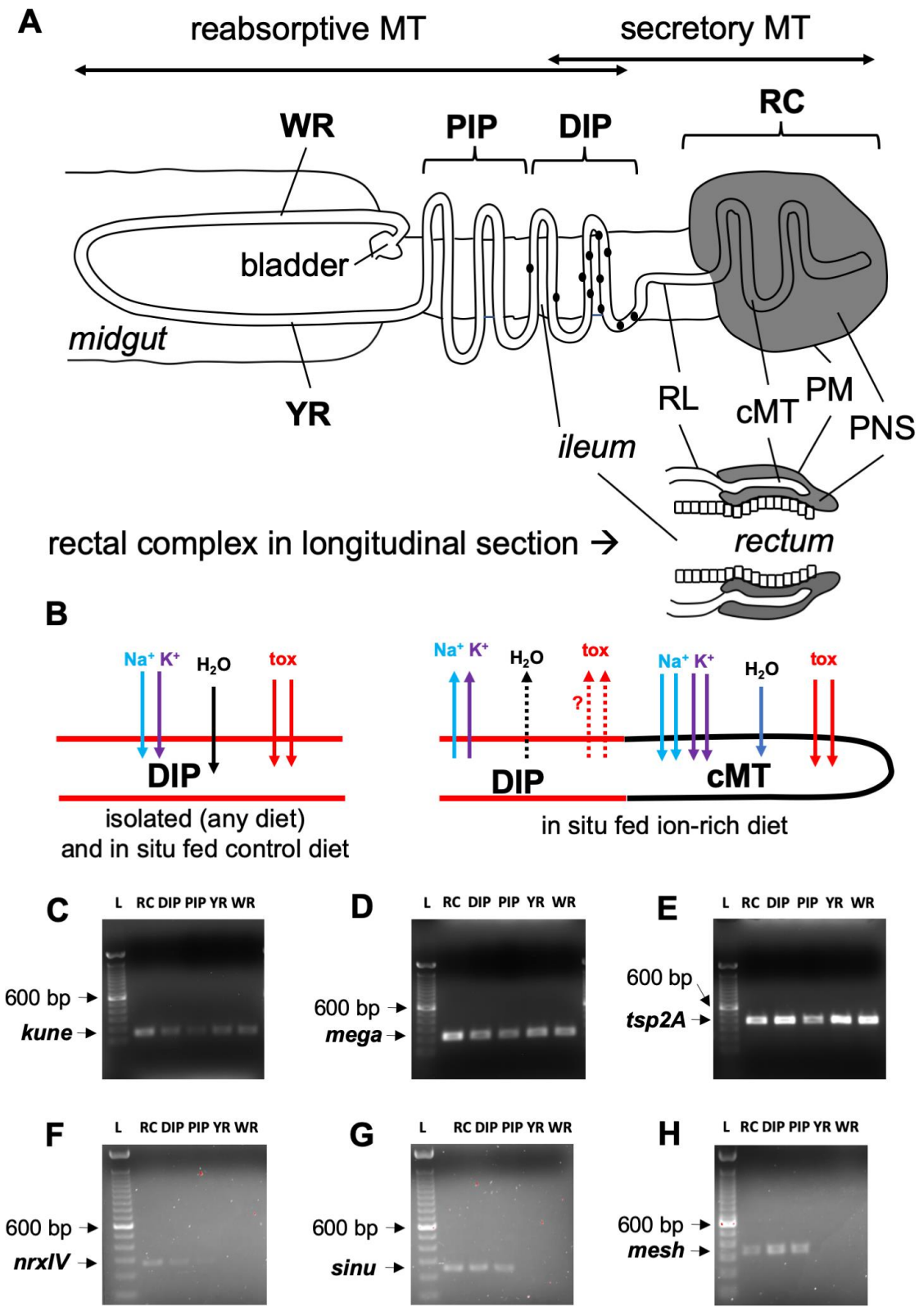

Figure 1 Septate junction gene transcript expression profile in the Malpighian tubule of larval *Trichoplusia ni*. (A) Diagram of excretory system components of the larval lepidopterans. The distal end of each Malpighian tubule, the cryptonephridial tubule (cMT), is embedded into perinephric space (PNS), and overlaid onto the underlying rectal epithelium and covered by the perinephric membrane (PM). This constitutes the rectal complex (RC). The rectal lead (RL) connects each cMT to the downstream tubule region, the ileac plexus. The distal ileac plexus (DIP) contains most secondary cells (solid black dots). The proximal ileac plexus (PIP) then terminates in the downstream yellow and white regions (YR and WR, respectively) that are closely applied to the posterior midgut, prior to terminating into the urinary bladder at the midgut-hindgut juncture. (B) Previous studies have shown that in situ DIP of larvae fed control diet, and isolated DIP of larvae fed any diet secretes ions (Na^+, K^+), fluid (H_2O), and organics (tox). In contrast, DIP of larvae fed ion-rich diets reabsorbs excess dietary ions, extracted from the gut by the rectal complex, and supplied into the tubule lumen by the upstream cMT. This switchover from ion secretion to ion reabsorption has been shown to be in part mediated in by the neuropeptide Helicokinin, which simultaneously reduces water permeability of the DIP to prevent the backflux of water. However, in order for the switch from secretion to reabsorption to be safe for the animal, presumably, reduced permeability to organics and toxins would have to be ensured as well. RT-PCR analysis of (C) *kune*, (D) *mega*, (E) *tsp2A*, (F) *nrxIV*, (G) *sinu*, and (H) *mesh* in the rectal complex (RC), distal ileac plexus (DIP) proximal ileac plexus (PIP), and yellow and white regions (YR and WR) of larval *T. ni* Malpighian tubule. In each panel, a 600 base-pair (bp) molecular weight band is indicated on the ladder (L) and all bands below it decrease by 100 bp increments.

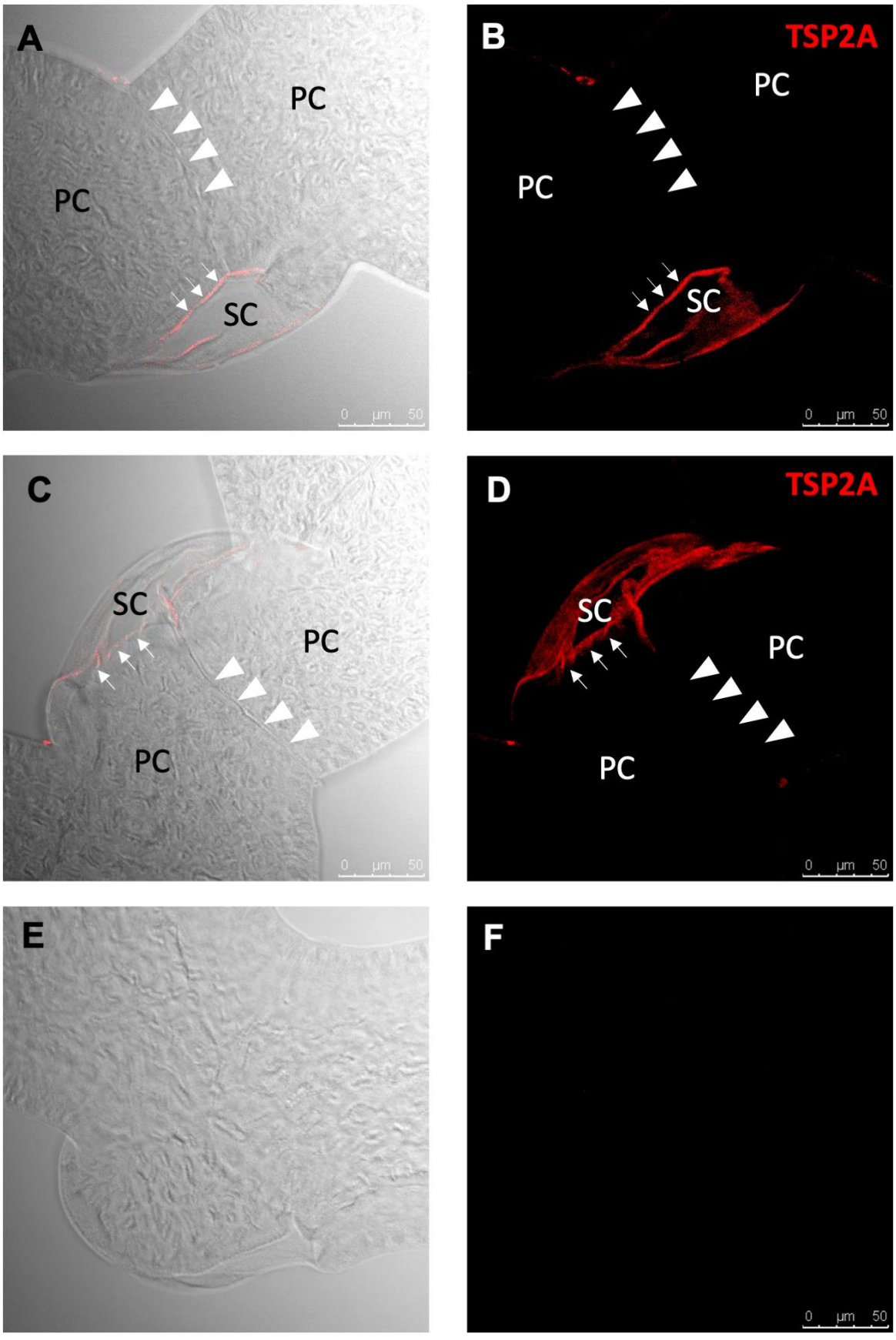

Figure 2 Immunofluorescence staining of Tsp2A in the distal ileac plexus of larval *Trichoplusia ni*. Tsp2A immunostaining appears to be confined to the contact regions between the principal and secondary cells (PC and SC, respectively; arrows in A-D), but is absent in the junctional regions between the two PCs (arrowheads in A-D). A and C show brightfield images of the areas shown in B and D, respectively. (E-F) Negative control preparation lacking primary antibody. Scale bars, 50 µm.

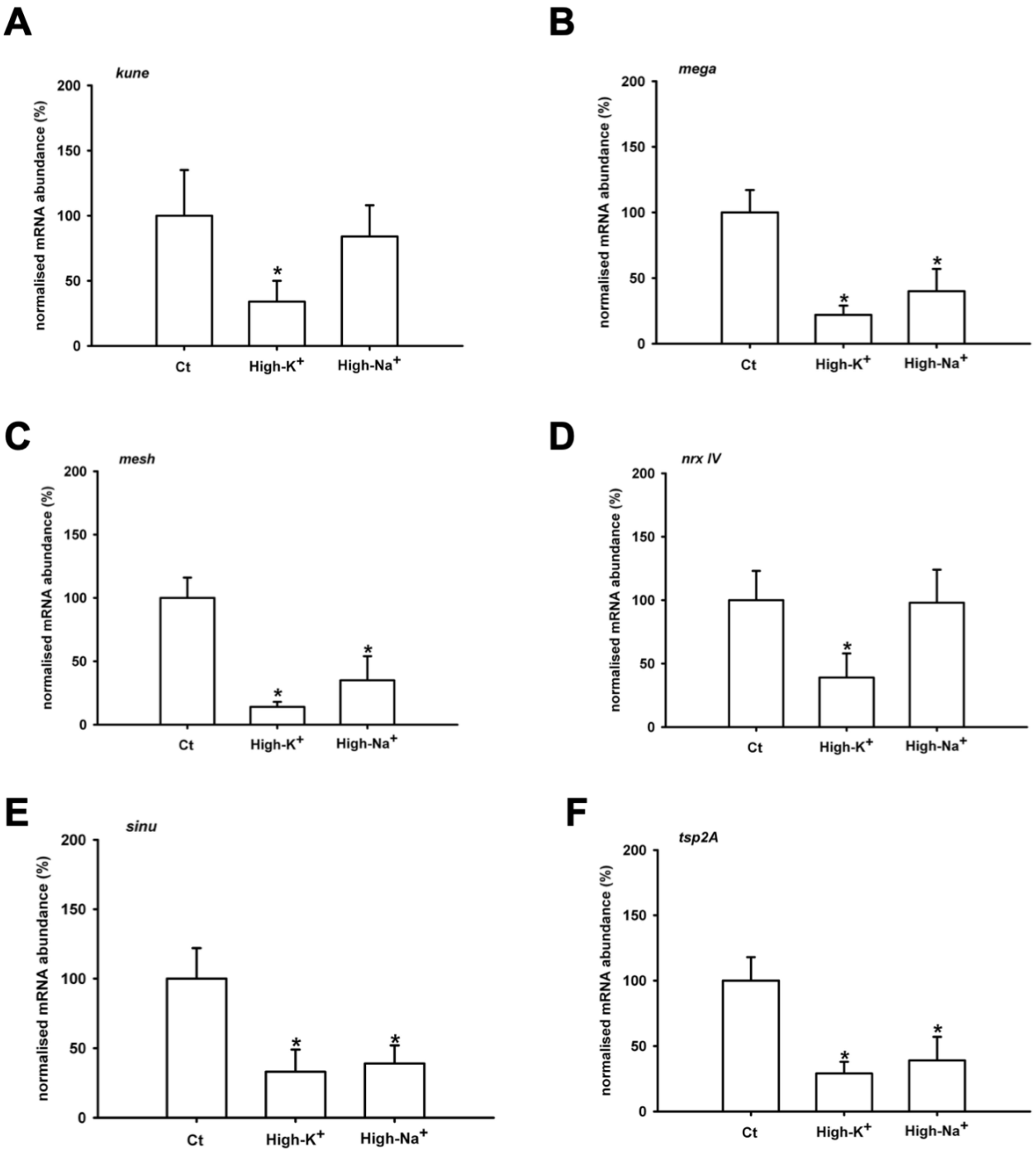

Figure 3 The effect of dietary ion loading on SJ gene transcript abundance in the distal ileac plexus (DIP) of larval *Trichoplusia ni*. Feeding fifth instar *T. ni* larva high-K^+ diet decreased transcript abundance of (A) *kune*, (B) *mega*, (C) *mesh*, (D) *nrxIV*, (E) *sinu*, and (F) *tsp2A* in the DIP. In contrast, feeding the animals high-Na^+ diet decreased transcript abundance of (B) *mega*,

(C) *mesh*, (E) *sinu* and (F) *tsp2A* only. All data are presented as mean values ± s.e.m. (N = 5). An asterisk indicates a significant difference from the control group as determined by one-way ANOVA coupled with a Holm-Sidak post-hoc test.

A

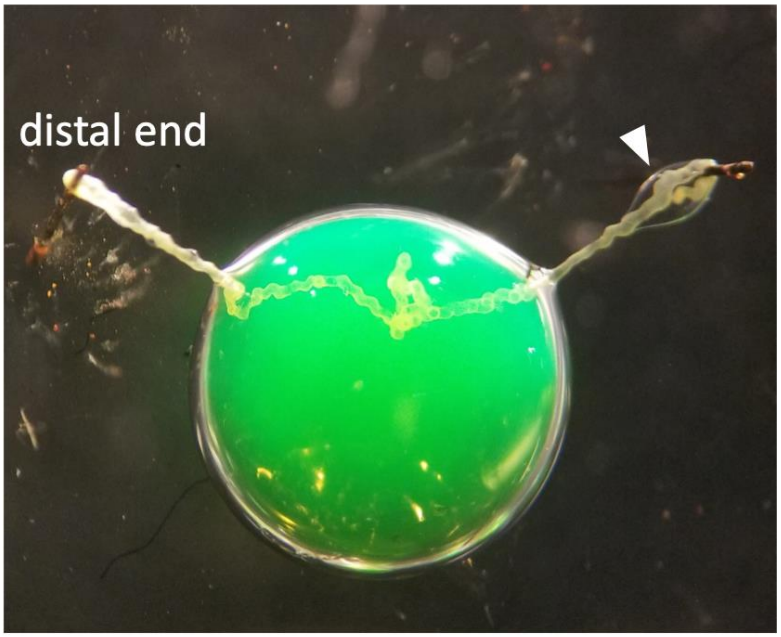

B

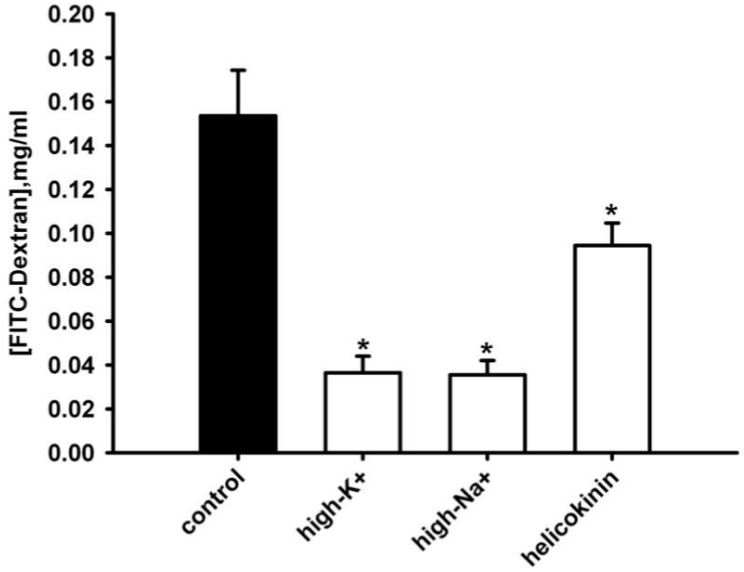

Figure 4 Effects of ion-rich diet and helicokinin (HK) on FITC-dextran permeability across the distal ileac plexus (DIP) of larval *Trichoplusia ni*. (A) Representative Ramsay preparation showing one tubule bathed in a 70 µl droplet of saline containing 3 mg/ml of 4 kDa FITC-dextran and a droplet of secreted fluid forming at the proximal end on the right pin (white arrowhead). (B) DIP from larvae fed ion-rich diets demonstrated reduced permeability to FITC-dextran, as did the DIP of control-fed larvae treated with 10^{-8} M HK in vitro. All data are presented as mean values ± s.e.m. (N=5). An asterisk denotes a significant difference from the control group as determined by Student's t-test ($P<0.05$).

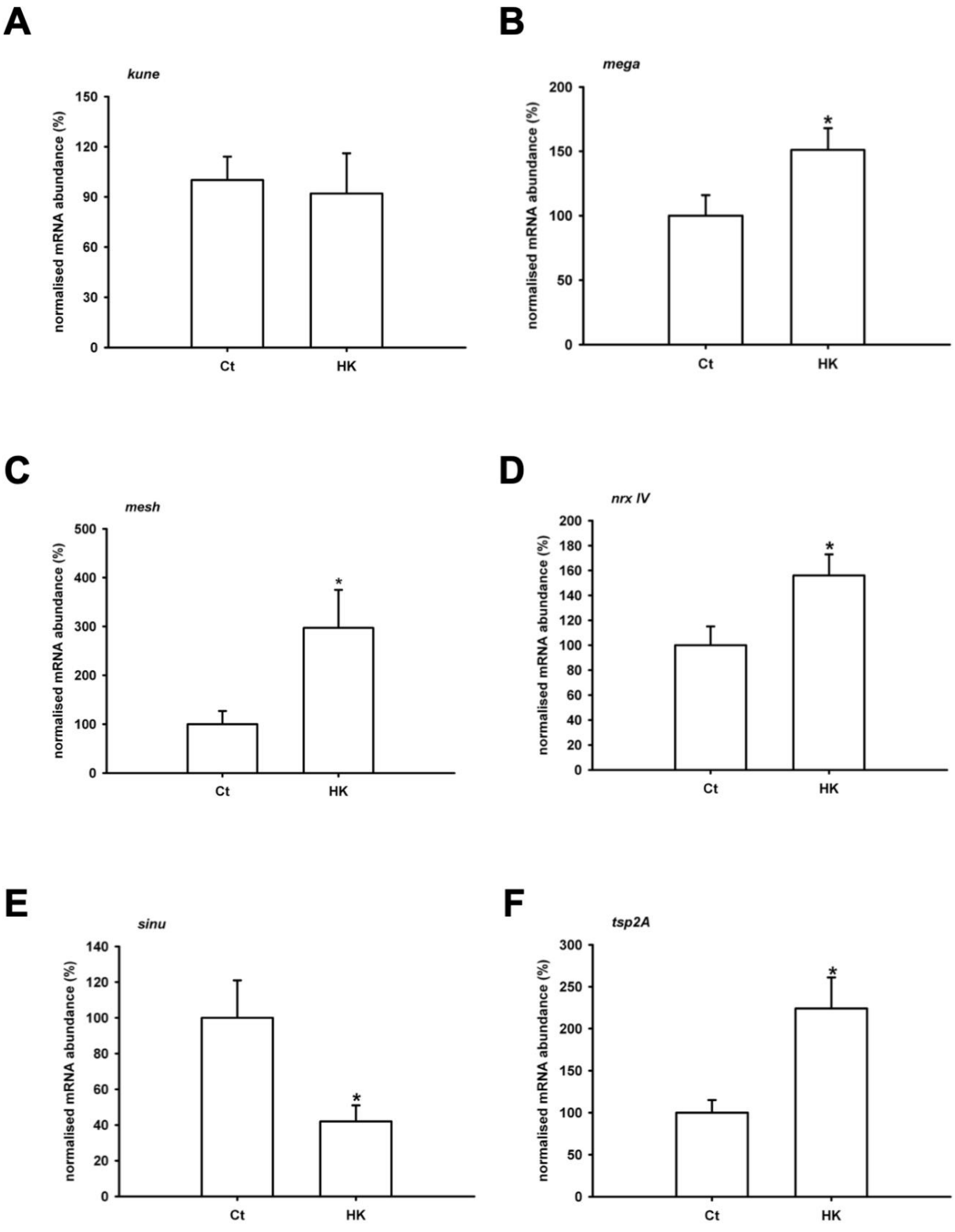

Figure 5 Effects of helicokinin (HK) on SJ gene transcript abundance in the distal ileac plexus (DIP) of larval *Trichoplusia ni*. 10^{-8} M HK treatment of DIP isolated from fifth instar *T. ni* larva fed on control-diet did not alter mRNA abundance of (A) *kune* but increased transcript abundance of (B) *mega*, (C) *mesh*, (D) *nrxIV*, and (F) *tsp2A*, and reduced mRNA abundance of (E) *sinu*. All data are presented as mean values ± s.e.m. (N=5). Asterisks indicates significant difference from the control group as determined by a Student's t-test ($P<0.05$).

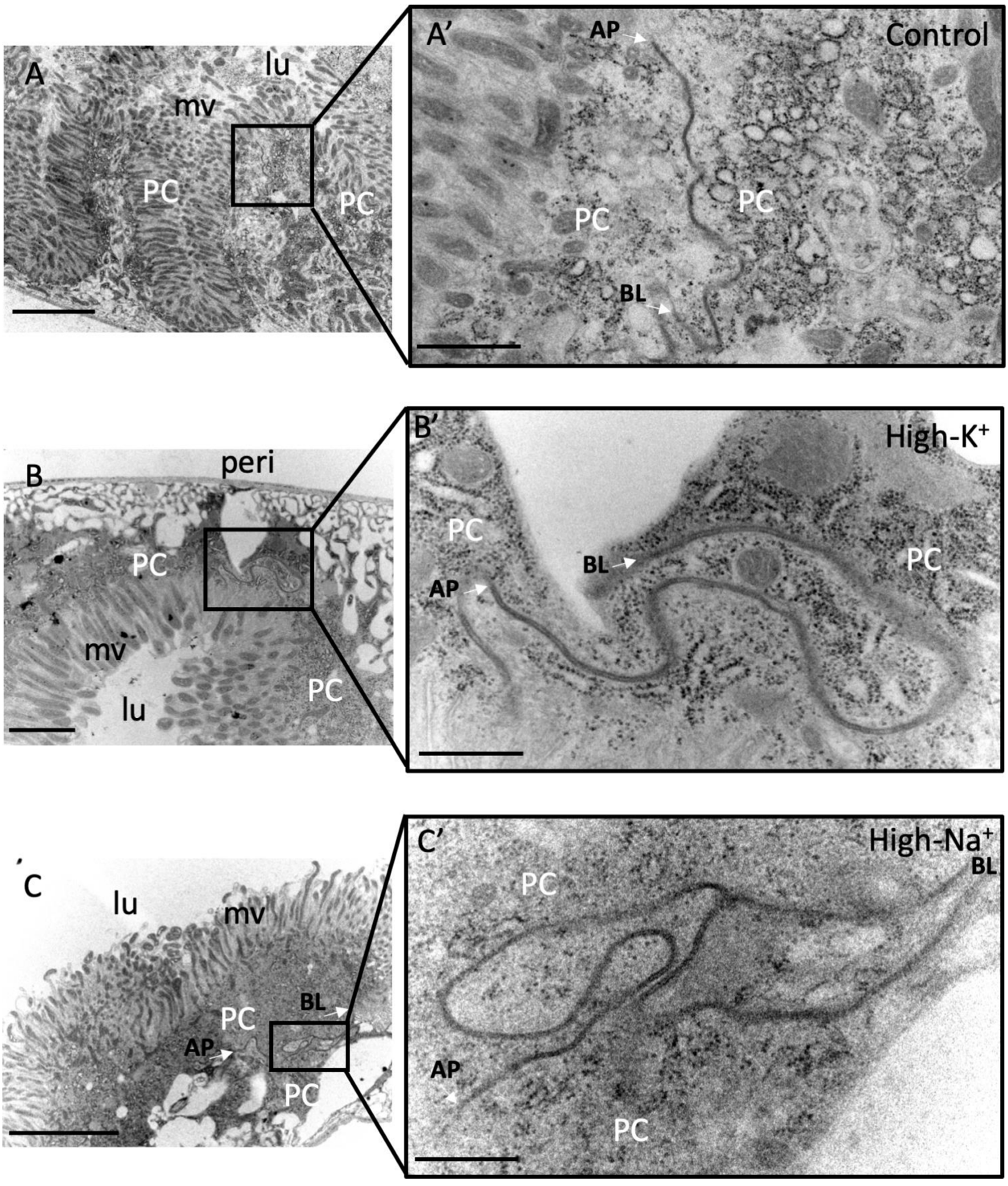

Figure 6 Effects of ion-rich diet on septate junction morphology between the principal cells (PC) of the distal ileac plexus (DIP) of larval *Trichoplusia ni*. Representative transmission electron microscopy images of DIP of larvae exposed to control (A-A') high-K^+ (B-B') and high

Na^+ (C-C') diets. The DIP epithelium of larvae fed ion-rich diets demonstrated longer and more convoluted SJs between adjacent PCs (B, C) compared to SJs of control group (A). Individual scale bars are provided in the bottom-left corner of every micrograph and their lengths denoted in the images. Scale bars: 5 µm in A and C; 2 µm in B; 1 µm in A'; 0.5 µm in B' and C'. White arrows are used to indicate the apical-most and the basal-most ends of the SJ. Panels A'-C' are higher magnification regions of panels A-C. AP – apical end of the SJ. BL – basolateral end of the SJ. Apical microvilli - mv, lumen - lu and peritubular space – peri.

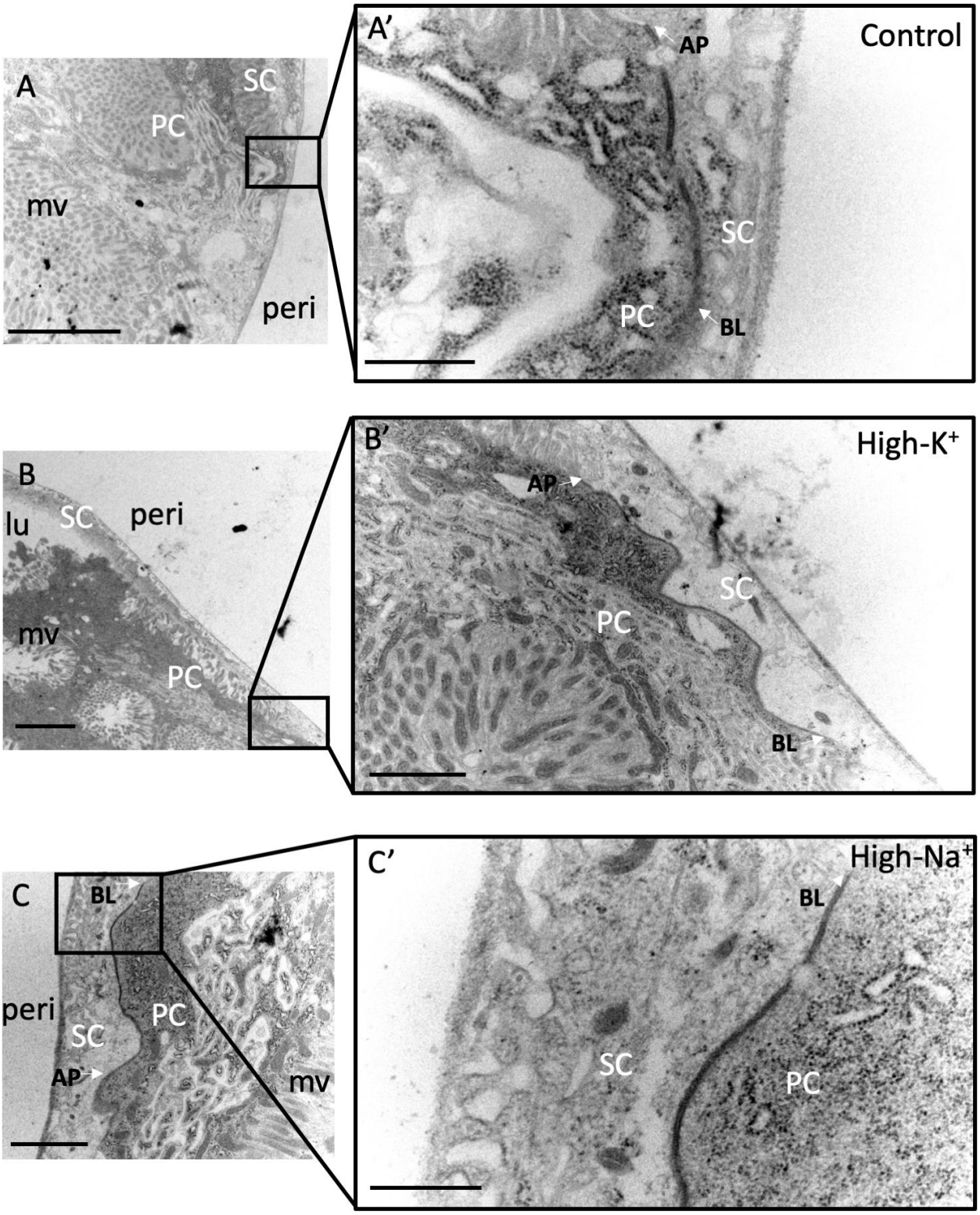

Figure 7 Effects of ion-rich diet on septate junction morphology between the principal cell (PC) and the secondary cell (SC) in the distal ileac plexus (DIP) of larval *Trichoplusia ni*. Representative transmission electron microscopy images of DIP of larvae exposed to control (A-A') high-K^+ (B-B') and high Na^+ (C-C') diets. PC and SC of DIP of larvae exposed to control, high-K^+ or high Na^+ diets demonstrated longer SJs. Individual scale bars are provided in the bottom-left corner of every micrograph and their lengths denoted in the images. Scale bars: 5 µm in A and B; 2 µm in C and B'; 0.5 µm in A' and C'. White arrows are used to indicate the apical-most and the basal-most ends of the SJ. Panels A'-C' are higher magnification regions of panels A-C. AP – apical end of the SJ. BL – basolateral end of the SJ. Apical microvilli - mv, lumen - lu and peritubular space – peri.

Table S1. Primer sets used for PCR and qPCR analysis of septate junction transcript expression and abundance

Gene transcript amplified	Forward primer	Reverse primer	NCBI accession number	T_a, °C
Kune-kune (*kune*)	AATTGCCTTCGTTAGTCCTTACTG	CTTCTTCAAATATCCACCAGCATC	MK015656	60
Megatrachea *(mega*)	GCAGGCTTATTTTTACTTCTGTCG	ATCAACCAACCAGGCAGCA	MK015657	61
Mesh (*mesh*)	AGACCACAACACGCTCAATG	ATCCACTGTCGCTTTCGTTC	MK015660	60
Neurexin IV *(nrxIV*)	GGACCTATTTGTGCTGACGAA	AATGCGAAGTGTTTCCCTTG	MK015661	60
Sinuous *(sinu)*	CCCTTGTTACTGTGGCATT	GCGTGGCAATCATAAAACC	MK015659	56
Tetraspanin 2A (*tsp2A*)	CTTGCGTTGTTCTGGACTTCTC	ATGGTAGCCTCCTCTTCTTCTTTC	MK015658	61